Behavioral/Cognitive

Signals from Single-Opponent Cortical Cells in the Human cVEP

Valerie Nunez, James Gordon, and Robert Shapley

¹Center for Neural Science, New York University, New York, New York 10003, and ²Psychology Department, Hunter College, The City University of New York, New York, New York 10065

We used the chromatic visual evoked potential (cVEP) to study responses in human visual cortex evoked by equiluminant color stimuli for 6 male and 11 female observers. Large-area, colored squares were used to stimulate Single-Opponent cells preferentially, and fine color-checkerboard stimuli were used to activate Double-Opponent responses preferentially. Stimuli were modulated along the following two directions in color space: (1) the cardinal direction, L-M or M-L of DKL (Derrington, Krauskopf, and Lennie) space; and (2) the line from the white point to the color of the Red LED in the display screen, which was approximately intermediate between the L-M and -S directions in DKL space in cone-contrast coordinates. The amplitudes of cVEPs to large squares were smaller than those to checkerboards, and the latency of the cVEP response to squares was significantly less than the checkerboard latency. The latency of cVEP responses to the squares varied little with cone-contrast unlike the steep reduction of latency with cone-contrast observed in responses to color checkerboard patterns. The dynamic differences between cVEPs to squares and checkerboards support the hypothesis that a distinct neuronal mechanism responded to squares: Single-Opponent cells. Response amplitude, latency, and transientness—and their dependence on cone-contrast—were similar in the responses in the L-M and Red color directions. The similarity supports the hypothesis that the Single-Opponent signals in the cVEP come from a distinct population of cells that receives subtractive inputs from L and M cones, either L-M or M-L.

Key words: color perception; cVEP; double-opponent cells; human visual cortex; Single-Opponent cells

Significance Statement

This article is about characterizing the visual behavior of a distinct population of neurons in the human visual cortex, the Single-Opponent color cells. Based on single-cell results in the visual cortex of macaque monkeys, we used large uniformly colored stimuli to isolate the responses of Single-Opponent cells in the chromatic visual evoked potential (cVEP) recorded on the scalp of human observers. VEP signals recorded under conditions believed to reveal Single-Opponent responses are small and transient. Their time course is relatively unaffected by cone-contrast, and they are relatively insensitive to stimulus modulation of short wavelength-sensitive S cones. Because Single-Opponent cells convey signals that can be used to judge the color of scene illumination, knowing their visual properties is important for understanding color vision.

Introduction

Human color perception is based on the responses to color by populations of neurons in the primary visual cortex (V1). Color signals are sent to the visual cortex first via the retinocortical pathway to V1 (De Valois, 1960; Derrington et al., 1984; Chatterjee and Callaway, 2003) and then V1 provides signals

Friedman et al., 2003; Johnson and Mullen, 2016).

Most of what we know about neuronal responses to color in V1 is based on research in macaque monkeys (Livingstone and Hubel, 1984; Thorell et al., 1984; De Valois and De Valois, 1988; Lennie et al., 1990; Johnson et al., 2001; Friedman et al., 2003; Hass and Horwitz, 2013; Garg et al., 2019). The results of the monkey experiments that are important for us here are that color-responsive neurons in macaque V1 can be assigned to the following two distinct groups: color-preferring (Lennie et al., 1990; Johnson et al., 2001) and color-luminance cell classes (Johnson et al., 2001; Hass and Horwitz, 2013). Most color-preferring cells are Single-Opponent cells, and color-luminance cells are mostly Double-Opponent cells (Johnson et al., 2004). In this article, we present evidence from recordings of the chromatic visual evoked potential (cVEP; Murray et al., 1987; Rabin et al.,

about color to extrastriate cortical areas (Kiper et al., 2001;

Received Feb. 4, 2022; revised Mar. 23, 2022; accepted Apr. 8, 2022.

Author contributions: V.N., J.G., and R.S. designed research; V.N., J.G., and R.S. performed research; V.N., J.G., and R.S. analyzed data; V.N., J.G., and R.S. edited the paper.

This research was supported by National Science Foundation Grant 1753846. We thank the following students who helped run the experiments: Afsana Amir, Chloe Brittenham, Patricia Pehme, Vera Pertsovskaya, and Ashlev Rosemond.

The authors declare no competing financial interests. Correspondence should be addressed to Valerie Nunez at valerie.nunez@nyu.edu. https://doi.org/10.1523/JNEUROSCI.0276-22.2022

Copyright © 2022 the authors

1994; Girard and Morrone, 1995; Crognale, 2002; Souza et al., 2008; Nunez et al., 2017, 2018) that human V1 also has Single-Opponent and Double-Opponent cells and that distinct cVEP components carry signals from one or the other group of color neurons.

Single-Opponent and Double-Opponent V1 neurons have quite different selectivities for spatial patterns of color (Johnson et al., 2001; Schluppeck and Engel, 2002). Single-Opponent cells respond best to red-green equiluminant color patterns with spatial frequency <0.5 cycles per degree (c/deg) and very little to color patterns >2 c/deg, while Double-Opponent cells are spatially tuned, responding best to red-green equiluminant patterns at 2 c/deg and very little to spatial frequencies <0.5 c/deg (Thorell et al., 1984; Lennie et al., 1990; Johnson et al., 2001; Schluppeck and Engel, 2002). Single-Opponent cells are low-pass filters, while Double-Opponent cells are bandpass filters, of spatial patterns of color (Thorell et al., 1984; Lennie et al., 1990; Johnson et al., 2001; Schluppeck and Engel, 2002). The different spatial properties allow us to stimulate only one class of color-responsive cells by choosing a pattern that is not visible to the other class. Thus, using as stimuli large, uniformly colored squares, we report in this article that it is possible to measure responses of the human Single-Opponent population in the cVEP and to characterize its distinctive response dynamics.

The combined action of Single-Opponent and Double-Opponent cells must be the basis for all aspects of color perception because they are the neurons in V1 that respond to color. The different spatial selectivities of Single-Opponent and Double-Opponent cells indicate that each group has a specific, distinct function in color vision, as suggested previously (Livingstone and Hubel, 1984; Shapiro et al., 2018; Shapley et al., 2019). The spatial tuning of Double-Opponent cells makes them sensitive to steep gradients of color near the boundaries of colored surfaces. In this way, the Double-Opponent neurons provide the signals that allow people to perceive the colors of colored-surfaces (Livingstone and Hubel, 1984; Friedman et al., 2003; Johnson et al., 2008; Nunez et al., 2018). Double-Opponent neurons have also been proposed as a possible source of the watercolor effect (Devinck et al., 2014; Cohen-Duwek and Spitzer, 2019; for review, see Devinck and Knoblauch, 2019). Single-Opponent cells may be important in judging the color of the illuminant of a scene and in detecting shallow spatial gradients of illumination color (Johnson et al., 2008; Nunez et al., 2018; Shapiro et al., 2018). The characteristics of spatial tuning of Single-Opponent neurons and their weighting of cone inputs revealed in the Results may have important consequences for the contextual effects that are so important in color perception (Krauskopf, 1963; Brainard, 2004), particularly color constancy (Foster, 2011).

Materials and Methods

Participants. All observers gave informed consent to participate in this study. The experiments were conducted in accordance with the principles embodied in the Declaration of Helsinki and were approved by the Hunter College/City University of New York and the New York University Institutional Review Boards.

A total of 17 observers participated in the study. Fifteen observers (six male, nine female; age range, 20–50 years; mean = 32.4, SD = 12.1) viewed stimuli in the Red color direction. Fourteen of those provided useable data for checkerboards, but only 8 gave measurable responses to uniform squares. The main reason for subject dropout (in data from five participants) was a noisy cable/electrode connection that affected the

data for those participants. The checkerboard responses were large enough to be seen clearly through the noise, so we used those data, but the small responses to the uniform square were masked by it so we had to exclude those. Once we improved the cable connection, we added participants to the study, hence the total of 15. Additionally, data from two participants who viewed the Red stimuli were excluded because of entrained alpha rhythms. There are uncontrollable individual differences in the propensity to generate alpha rhythms in response to visual stimuli.

Eight observers (one male, seven female; age range, 21–51 years; mean = 27.3 years, SD = 10.8) viewed the L-M stimuli. All eight gave measurable responses to the uniform square stimulus, but only seven of those gave measurable data for the checkerboard stimulus. The eight observers who viewed the L-M stimuli also viewed the stimuli in the S-cone-isolating direction.

There were six observers who viewed patterns in both L-M and Red color directions. Of those, all six gave useable data for both L-M and M-L. In the Red direction, five of six gave useable data for the large-area Red squares, and a different five of six gave useable data for the Red checkerboards.

All participants had normal color vision, assessed with the following: pseudoisochromatic plates; the Farnsworth dichotomous D15 hue test; Lanthony's desaturated 15 hue test; and the Farnsworth–Munsell 100-hue test. The participants also had at least 20/20 (or corrected to 20/20) visual acuity.

Apparatus. An organic LED (OLED) monitor (model PVM-A170, Sony) was used to present the stimuli. The monitor had a diagonal screen size of 42 cm (effective picture size, 365.8×205.7 mm, which at the viewing distance of 114 cm corresponded to $18.3^{\circ} \times 10.3^{\circ}$ visual angle), a resolution of 1920×1080 , and a frame rate of 60 Hz. The screen was calibrated using a PR670 SpectraScan Spectroradiometer/Photometer (Photo Research) to calculate gamma corrections for the individual red, green, and blue LEDs to ensure complete control of intensities on the screen.

Visual stimuli. The following two kinds of color stimuli were used: color checkerboards and uniformly colored squares with blurred edges. The checkerboard pattern consisted of a small central colored checkerboard surrounded by an area in which the colored checks faded outward gradually to the background gray of the screen. The central checkerboard was 3.75 × 3.75 cm, corresponding to 1.875° × 1.875° of arc and had 8 × 8 checks, giving a dominant spatial frequency of 3.02 c/deg, slightly above the peak of the cVEP spatial frequency response reported by Rabin et al. (1994), but well below their recorded cutoff frequencies. Colored squares were also used to study the sensitivity of the cVEP to color stimuli without much spatial structure. These were the same size as the central checkerboards and were also surrounded by a color-fade area. Sample checkerboard and uniform-square stimuli are provided in Figure 1. For both checkerboards and colored squares, the fading transition from maximum color at the edge of the central square to zero color (i.e., the gray background) occurred as a Tanh function, with a width of 3.75 cm. Therefore, including the outer fade area, there was some degree of color subtending a total angle of 5.625°, though color was reduced by a factor of 2 within a total angle of 3.75°.

The background color of the screen was approximately equivalent to that of equal-energy white. For experiments in the Red direction, the gray background had a luminance of 32.1 cd/m^2 , an equivalent color temperature of 5786° , and CIE x–y coordinates of (0.326, 0.341). In the L-M and in the S direction, the background had a luminance of 30.2 cd/m^2 , a color temperature of 5790° , and CIE coordinates of (0.326, 0.340).

For the Red direction, pattern color was from a range of contrasts along the direction of the Red screen LED. For the L-M direction, the pattern color was from a range of cone-contrasts in the L-M direction of DKL (Derrington, Krauskopf, and Lennie) space (Derrington et al., 1984). In the L-M direction, the excitation of L cones relative to the background was equal and opposite to the excitation of M cones, but S cones were not excited. For the S direction, the pattern color was from a range of cone-contrasts in the S-cone-isolating direction, where the L and M cones were not excited relative to the background. As all stimuli were equiluminant with the background, there was no luminance

modulation. For the initial Red check stimulus (Fig. 1A), the first check color was a contrast in the Red color direction and the second check was the same color as the gray background. For the remaining checkerboard stimuli, the first check color was in one of the color directions (Red, L-M, or S); the second check was the complement of the first, so that spatially averaged color over the entire checkerboard was the background gray. To obtain the complement of a color for a participant, it was first ensured that the color was equiluminant with the gray background for the participant (see the section Heterochromatic flicker photometry). The complement was then calculated as what would have to be added to the color to result in the background gray. Spatial averaging to the background gray was evident when one stepped away from the screen. When individual checks were no longer discernible, the color-complement checkerboard merged into the gray background. Sample stimuli for each color direction are presented in Figure 1.

The contrasts of the stimulus colors are presented in Table 1. The L, M, and S-cone-contrasts in Table 1 were calculated as the ratio of differential cone excitation (difference in cone excitation between color and background) divided by the excitation caused by the background. The excitatory drive for the parvocellular pathway was L-M contrast, as shown in Table 1. The koniocellular pathway was driven by S-cone-contrast. For intermediate directions, for instance the Red direction, the magnitude of stimulus contrast was calculated as $\sqrt{(L-M)^2+S^2}$, the length of the stimulus vector in a vector space with axes |L-M| and |S|.

Figure 2 presents the loci of the stimuli in color space. The CIE x–y color coordinates of the stimulus colors, their complements, and the background gray, are presented in Figure 2A. Color-complement checkerboards were presented at several different cone-contrast levels up to the maximum possible within the gamut of the screen for each color direction. The stimulus colors are also represented in DKL space (Derrington et al., 1984) in cone-contrast coordinates in Figure 2B. Note that

the DKL space in Figure 2*B* plots the distance along the cardinal directions in cone-contrast coordinates in both the S and L-M directions (Brainard, 1996; Wuerger et al., 2005). While the L-M color direction was chosen to isolate responses from the parvocellular pathway, the "Red" color direction corresponded to the color direction of the Red primary of the OLED screen. From Figure 2*B*, it is evident that stimuli along the Red color direction should produce a combination of responses from both L-M and S-cone-driven mechanisms (but see Nunez et al., 2021).

For each stimulus, the screen would cycle between the gray background and the color pattern. This cycle was a 0.5 s period of background gray, followed by 0.5 s of pattern appearance, then 1.0 s of background gray, (rectangular-wave, appearance–disappearance modulation), resulting in a period of 2.0 s, a frequency of 0.5 Hz, and a duty cycle of 25%.

Stimulus presentation was controlled using the Psychophysics Toolbox extensions (Brainard, 1997; Pelli, 1997; Kleiner et al., 2007) for MATLAB R2012b, which is detailed in the study by Nunez et al. (2017).

Heterochromatic flicker photometry. The equiluminance of each stimulus color compared with the background gray was determined for each participant with heterochromatic flicker photometry (HFP). A

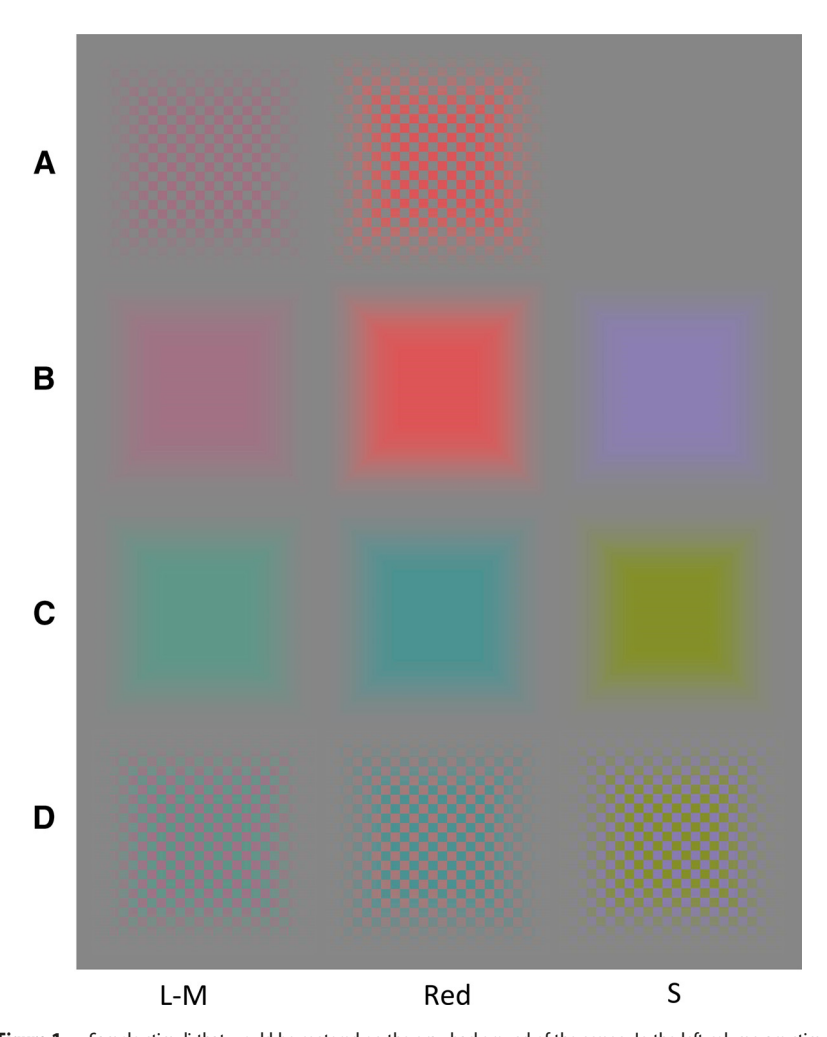


Figure 1. Sample stimuli that would be centered on the gray background of the screen. In the left column are stimuli in the L-M direction; in the middle column are stimuli in the Red direction, a color direction between the L-M and S axes; and in the right column are stimuli in the S direction. In row A, a central 8×8 color-gray checkerboard is surrounded by a checkered region that fades gradually to the background gray. In row B, a uniform-colored square of the same central size as the checkerboard is surrounded by a colored region that fades gradually to the background gray. In row C, the colored region is the complement of the color in row B. Row D shows checkerboards of the color and its complement. The central, highest-contrast region of each pattern spanned 1.875° \times 1.875°. All colors were equiluminant with the background for each participant.

Table 1. Cone-contrast (defined as differential cone excitation of stimulus color from background gray divided by excitation because of background) and the contrast measures used to describe each stimulus color presented

	Cone-contrast			Contrast measure		
Color direction	L	М	S	L-M	S	$\sqrt{\left(L-M\right)^2+S^2}$
L-M	0.015	-0.028	-0.008	0.043	0.008	0.044
	0.036	-0.056	-0.010	0.093	0.010	0.093
	0.045	-0.092	-0.001	0.137	0.001	0.137
	0.054	-0.124	0.002	0.178	0.002	0.178
	0.084	-0.133	-0.011	0.218	0.011	0.218
Red	0.015	-0.035	-0.055	0.050	0.055	0.074
	0.021	-0.053	-0.089	0.075	0.089	0.116
	0.034	-0.079	-0.131	0.113	0.131	0.173
	0.041	-0.097	-0.163	0.138	0.163	0.214
	0.044	-0.116	-0.191	0.160	0.191	0.249
	0.055	-0.129	-0.219	0.183	0.219	0.286
	0.068	-0.148	-0.258	0.216	0.258	0.336

The two color directions were the L-M cardinal axis of DKL space, and the Red direction was from the white point along the direction of the red LED of the screen.

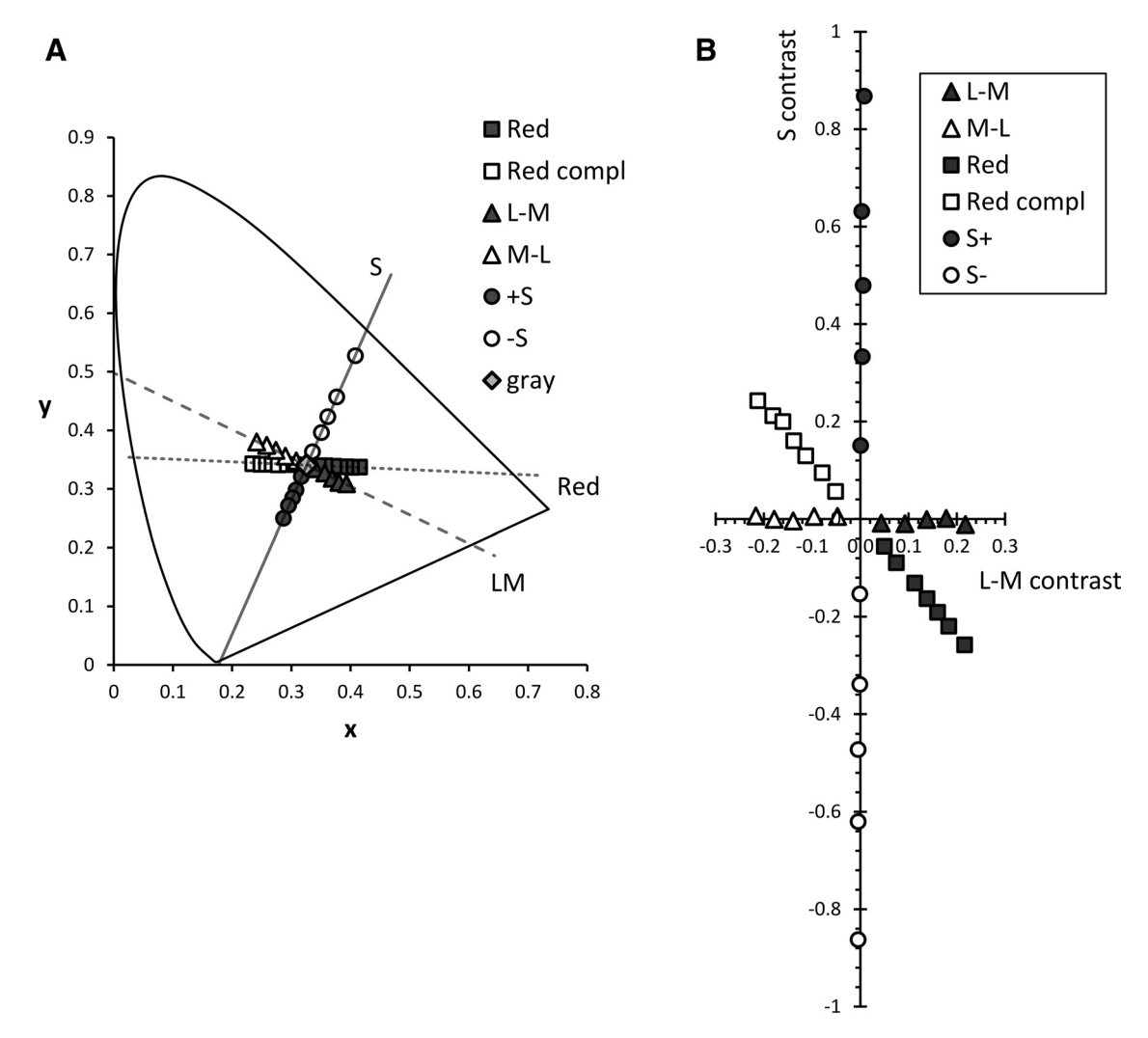


Figure 2. A, CIE x—y color coordinates of the stimuli used and the background gray. The dashed line labeled LM corresponds to the L-M color direction, and the solid line labeled S corresponds to the S color direction. The dotted line labeled Red corresponds to the color direction of the red primary of the OLED screen. **B**, Cone-contrasts of the color stimuli in the three color directions used in experiments. The x-coordinate is the L-M contrast, and the y-coordinate is the S-cone-contrast.

central color square or color-gray checkerboard of the same size and spatial frequency as the stimuli (but not fading to background) was exchanged with background at a frequency of 15 Hz. The radiance of the color that produced minimum flicker was recorded and averaged over 12 repeats to determine the luminance match.

Procedure. During each experiment, the participant was seated such that their eye level was aligned with the center of the screen and the viewing distance was 114 cm. Stimuli were viewed binocularly. There was one block of 30 stimulus presentations for each pattern, color direction, and cone-contrast combination; blocks were presented in random order. Each participant was asked to focus on the center of the screen and to blink as little as possible, particularly when a stimulus was visible on the screen.

Data acquisition and analysis. Data were recorded using an ActiveTwo System (BioSemi) as detailed previously (Nunez et al., 2017). The trigger and EEG signals were sampled at a frequency of 2048 Hz, with an open passband from 0 to 400 Hz. The topography of the cVEP for a participant viewing a color checkerboard is presented in the study by Nunez et al. (2017, their Fig. 4), where the cVEP was confined in space on the scalp to the most posterior electrodes over V1 cortex. All the data reported in this article were measured at electrode Oz, corresponding to the largest cVEP responses (Nunez et al., 2017).

Please see Nunez et al. (2017) for details of the analysis pipeline. Data were separated into trials containing a prestimulus period of 100 ms and a poststimulus period of 1000 ms and were linearly detrended before

being baseline corrected with respect to the average voltage of the prestimulus period. However, four participants who blinked repeatedly after the stimulus disappeared had their poststimulus period restricted to the 500 ms when the stimulus was on-screen. Waveforms reconstructed from the inverse discrete Fourier transform were low-pass filtered to 50 Hz.

In examining the waveforms to calculate latency, amplitude, and transientness as functions of contrast, we observed that some participants did not produce measurable responses for some contrasts (either because of the contrast being too low for the participant or because of the data being contaminated by noise or alpha waves). In those cases, the individual data for those pattern–contrast combinations were removed from the full dataset. For the Red uniform square pattern, so few participants produced evident responses for the lowest contrast that all the data with that contrast were excluded from the dataset. There were also participants for whom the highest Red contrast did not have a complement within the gamut of the screen (following adjustments for HFP). In that case, the minimum number of participants included in an average for that contrast was five.

Results

cVEP waveforms

cVEP responses to color-gray checkerboards

The first inkling we received that human Single-Opponent signals could be found in the cVEP was when we used color-gray

checkerboards, like those illustrated in Figure 1A, as stimuli for the cVEP (Nunez et al., 2017). In those previous experiments, the color-gray checkerboard pattern was composed of color checks alternating with gray checks, and all checks were equiluminant with the background; only the color checks were modulated in time. The fundamental spatial frequency of the checkerboard was chosen to be around the peak of cVEP responsiveness, ~2 c/deg (Rabin et al., 1994). But because it was a color-gray checkerboard, there was a space-averaged color to the checkerboard, a spatial DC signal. The cVEP was dominated by the large negative peak at 140-150 ms after stimulus onset, a signal that is understood to come from color-responsive neurons that are spatially tuned (Murray et al., 1987; Rabin et al., 1994; Crognale, 2002; Souza et al., 2008; Nunez et al., 2017, 2018)—the neurons that we have called Double-Opponent cells (Johnson et al., 2004, 2008; Shapley et al., 2019) following Livingstone and Hubel (1984). But, in the cVEPs responding to color-gray checkerboards, there was also a smaller negative wave that peaked at ~100 ms, earlier than the Double-Opponent cVEP. These early peaks can be seen in the cVEP waveforms plotted in gray in Figure 3, for 3 c/deg colorgray checkerboards. Note that after the initial early negative peak in the color-gray responses, the response begins to relax back to the baseline, and then the larger, later negativity evoked by the checkerboard pattern dips down. It might appear that the early negative response is followed by a positive wave, but we think instead that the colorgray cVEP is simply the sum of two separate negative waveforms: an early one with a peak at 90 ms and a later one with a peak at between 140 and 200 ms (depending on cone-contrast).

The early 90-100 ms negative peak was present only when there was a spatial average color to the checkerboard pattern. It was absent in cVEP responses to 3 c/deg checkerboards composed of alternating color checks and their color complements (all checks equiluminant with background and all checks modulated in time), like the color-complement checkerboard patterns illustrated in Figure 1, row D. In such color-complement checkerboards, the space-averaged color is the same gray as the background. In other words, the color and complement checks sum to mid-gray if you average over one cycle of the checkerboard. That means there is no effective stimulus for the Single-Opponent cells in such stimuli at spatial frequencies of the checkerboard >1 c/deg. If the early peak is a sign of the Single-Opponent population, we would expect the early peak to be absent in cVEPs to mid-to-high frequency color-complement checkerboards, and that is what happens (Fig. 3).

The absence of the early 90–100 ms peaks in color-complement checkerboard stimuli is illustrated in Figure 3 in the cVEP waveforms drawn as dashed lines. We reasoned that the color-complement checkerboard stimuli evoked only responses in Double-Opponent cells; the checkerboards were not spatially resolvable by the Single-

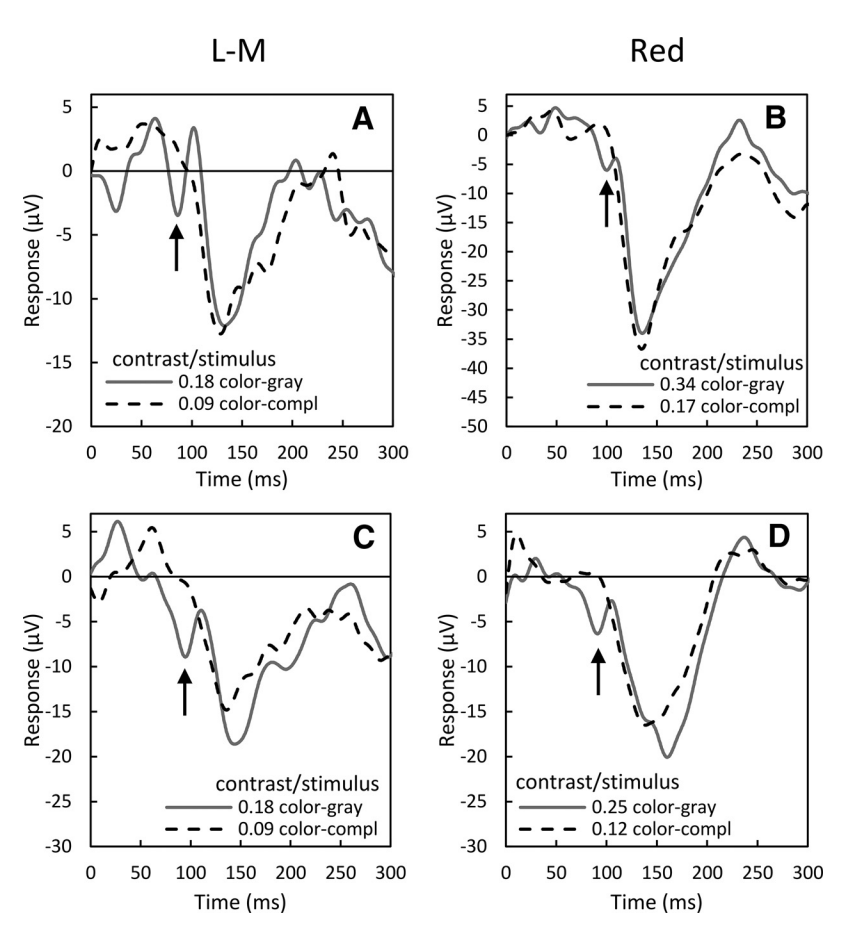


Figure 3. Sample waveforms for color-gray (gray solid line) and color-complement (black dashed line) checkerboards for a few different participants and contrasts, showing an early peak for the color-gray checkerboard but not for the color-complement checkerboard. A-D, In the first column (A, C), the stimulus was in the L-M color direction, and in the second column (B, D), the stimulus was in the Red color direction of the Red LED of the screen. In each plot, the color contrast of the color-gray stimulus is approximately double that of the color-complement stimulus, leading to equal space-averaged absolute contrasts. The contrasts indicated are the contrast measure $\sqrt{(L-M)^2+S^2}$.

Opponent population (Schluppeck and Engel, 2002). The color-gray checkerboards could and probably did excite both Single-Opponent and Double-Opponent cells. The waveforms in Figure 3 are from different participants and from L-M and Red color directions (see Materials and Methods; Fig. 2), proving that the early 90–100 ms negativity (Fig. 3, arrows) was a consistent feature of the cVEP when color-gray checkerboards were used and was consistently absent in responses to color-complement checkerboards. It is likely that previous studies that used equiluminant color grating patterns to evoke cVEPs (Murray et al., 1987; Rabin et al., 1994; Crognale, 2002; Souza et al., 2008) did not observe the 90-100 ms component that is evident in Figure 3 because most of the stimuli they used did not excite Single-Opponent cells; the grating stimuli had no space-averaged color, and, except for the lowest spatial frequencies used, the grating pattern would have been too fine for the Single-Opponent cells to resolve (Schluppeck and Engel, 2002).

cVEP waveforms in responses to large-area stimuli

The results with color-gray checkerboards in Figure 3 led us to study the cVEP patterns chosen to be optimal for stimulating cortical Single-Opponent cells. Such stimuli were large areas of

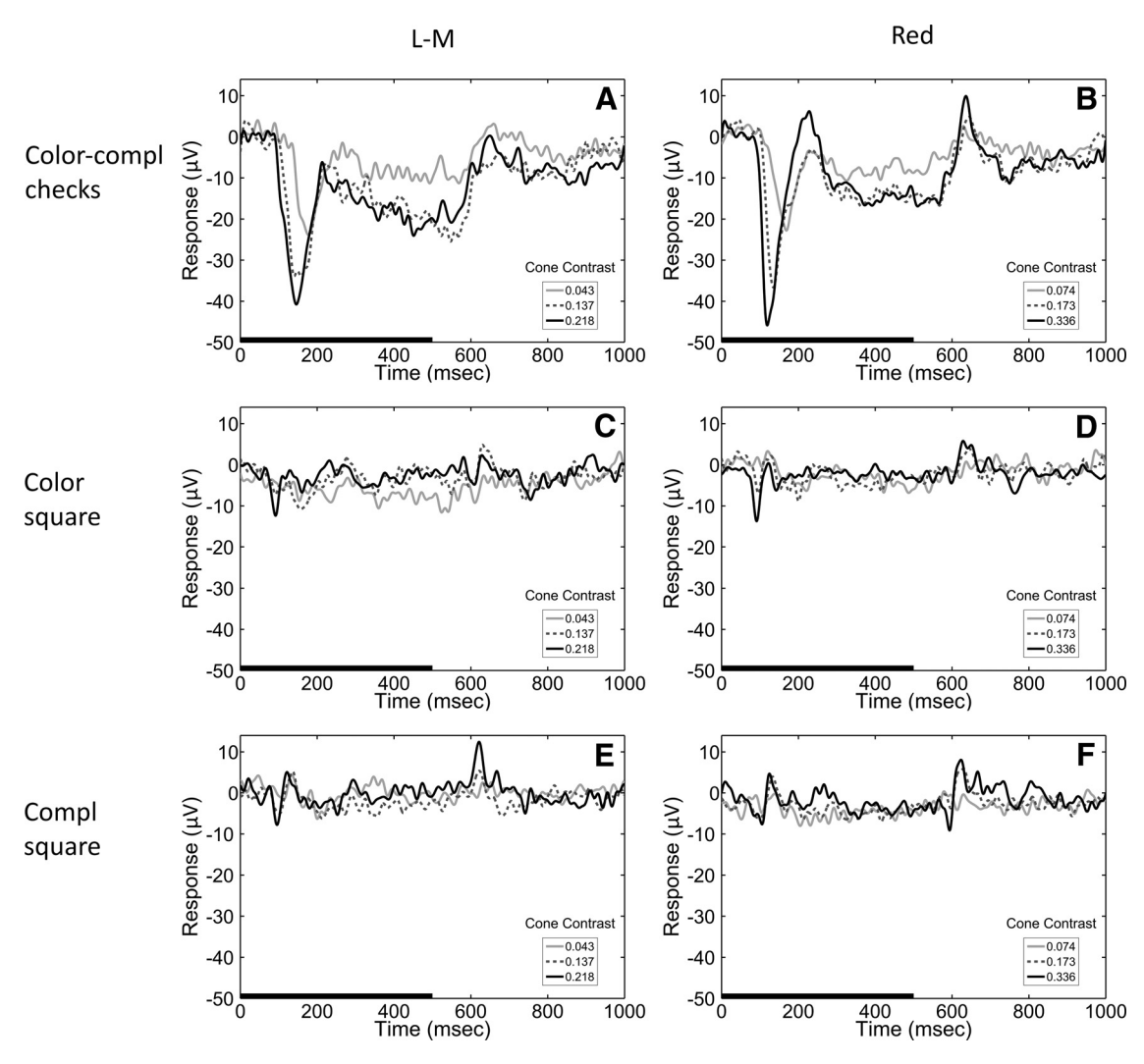


Figure 4. A–F, The cVEP waveform at electrode 0z for one participant observing different stimuli in the L-M (first column: **A**, **C**, **E**) and Red (second column: **B**, **D**, **F**) color directions. The top row shows responses from color-complement checkerboards for the L-M (**A**) and Red (**B**) color directions. The other two rows are responses to uniform squares of either the given color (**C**, **D**, middle row) or the complement of that color (**E**, **F**, bottom row). Specifically, the stimulus colors were in the following color directions: L-M (**C**), M-L (**E**), Red (**D**), and Red complement (**F**). For all stimuli, responses are plotted for a range of cone contrasts, covering the time period from pattern onset to 1000 ms after pattern onset. Note that the pattern was visible only for the first 500 ms, represented by the thick black bar along the time axis. Some of the data in the plots in **A–D** are similar but not identical to the data in the study by Nunez et al. (2021, their Fig. 3).

color with no sharp edges like those shown in Figure 1, rows B and C.

The waveforms of responses to large-area stimuli with blurred edges and to relatively fine checkerboards look very different (Fig. 4). Figure 4 shows cVEP data for one participant responding to patterns and large areas of color. The following two color directions were used: the cardinal red-green direction, which we will denote as L-M (or M-L), and the Red (and Red-complement) direction (see Materials and Methods; Fig. 2). The responses to checkerboards (Fig. 4A,B) have a characteristic large negative transient with peak negativity occurring at \sim 140–200 ms. The peak time is later at low cone-contrast (Murray et al., 1987; Rabin et al., 1994; Crognale, 2002; Souza et al., 2008; Crognale et al., 2013; Nunez et al., 2017, 2021). There was a sustained component of response to the appearance of the checkerboard that lasted for the duration of the stimulus and slightly longer in time (Nunez et al., 2021). However, the responses to the large-area squares plotted in Figure 4C-F are very different. The initial negativity occurs earlier, at \sim 90 ms; the response is much smaller in amplitude than the checkerboard response and

is very transient. Furthermore, the time of occurrence of the early negative peak is approximately invariant with cone-contrast. The responses to the L-M square (Fig. 4C) and to the M-L square (Fig. 4E) look very similar to each other, as do the responses to the Red square (Fig. 4D) and its complement (Fig. 4F). Large equiluminant color stimuli have been reported to generate early negative VEPs with peak negativity at 87 ms (Paulus et al., 1984), similar to those shown in Figure 4C-F.

Differences between the cVEPS to checkerboard and square with blurred edges were seen in the data from all participants. More comparisons of waveforms are presented in Figure 5 for three participants (labeled as P1, P2, and P3). In Figure 5, for each participant, cVEPs to large-area squares modulated in L-M, M-L, Red, Red-Complement (labeled "Compl") color directions are drawn in each column, in gray. The response of the same observers to L-M/M-L checkerboard stimuli are drawn in black in the bottom panel of each column (Fig. 5). As in the data shown in Figure 4, the large-area square stimuli evoked smaller, earlier negative peaks, and the entire response to the large-area squares was more transient than the checkerboard response. The

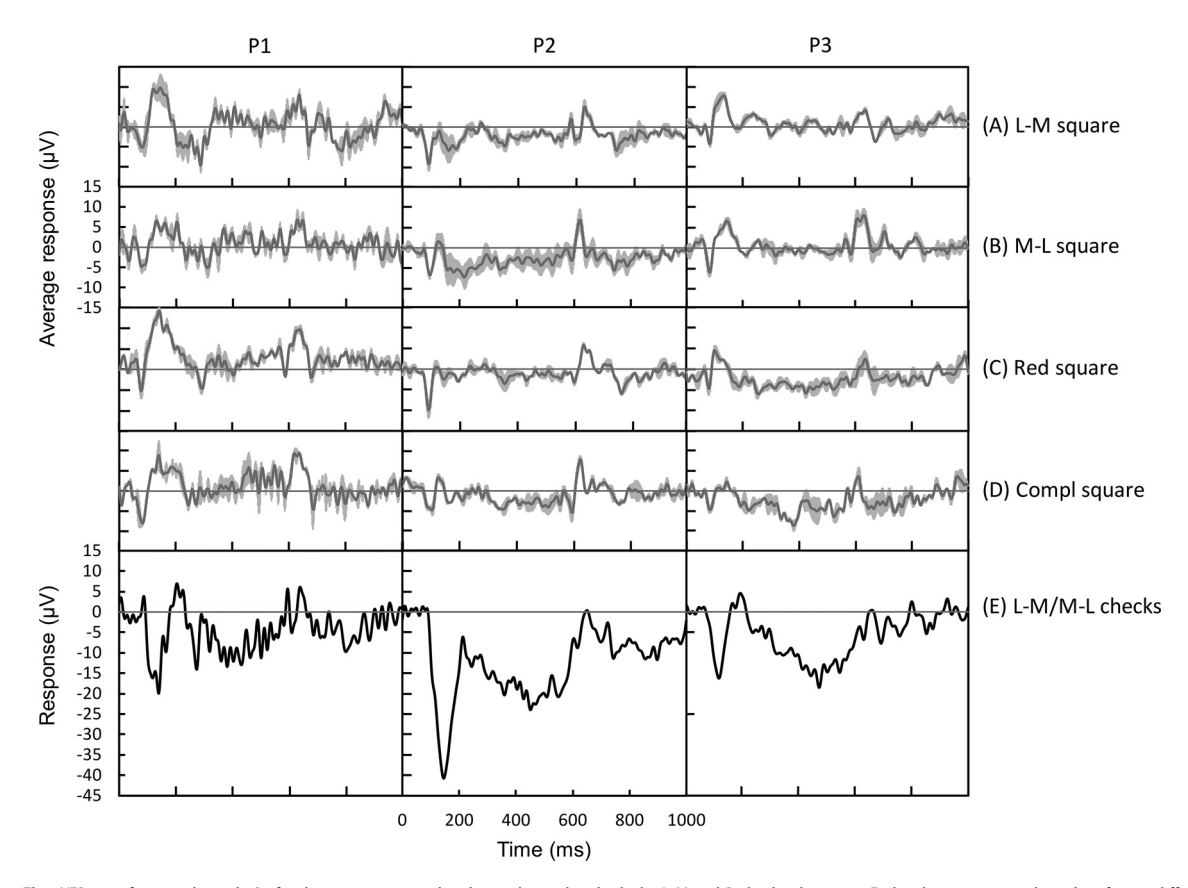


Figure 5. The cVEP waveform at electrode Oz for three participants who observed stimuli in both the L-M and Red color directions. Each column corresponds to data from a different participant (P1, P2, P3). The first four rows (gray) are responses to uniform-square stimuli, averaged over the top four contrasts in each case, all with the same vertical axis range. The error bars represent 1 SEM. The top row (**A**) shows contrast-averaged responses to a uniform square in the L-M direction, while the second row (**B**) is the contrast-averaged response to the complement M-L. Contrast-averaged responses to uniform squares of Red and its complement are presented in rows **C** and **D**, respectively. The bottom row (**E**; in black) is the response to the highest contrast color-complement checkerboard in the L-M direction. The vertical axis in row **E** has the same scale as rows **A-D** but requires a wider axis range to cover the larger response magnitudes of the color-complement checkerboards.

striking qualitative differences between the cVEPs evoked by colored patterns (Figs. 4A,B, 5) and those evoked by large-area stimuli (Figs. 4C-F, 5) suggest the existence of a functional dichotomy in early visual cortex: Single-Opponent and Double-Opponent cell populations. Quantitative analysis of the cVEPs to large colored areas, the putative Single-Opponent population responses (see Figs. 7-9), provides more support for a functional dichotomy.

S-cone-driven cVEP responses to large squares

The S-cone-driven cVEP to large-area stimuli was not measurable in most participants in these experiments. If there was a signal, it was lost in the noise. There were measurable cVEPs in response to large-area S-cone modulation for only two participants, P2 and P4. cVEP response waveforms for these two participants are plotted in Figure 6 and are compared there with S-cone-driven checkerboard responses. All of the cVEPs shown in Figure 6 were in response to the highest S-cone contrast used in the experiments, 0.87 (Fig. 2). The S-cone-driven checkerboard waveforms are like those we have reported previously (Nunez et al., 2021) and were observable in all participants' cVEPs, not only those illustrated in Figure 6. The cVEPs for large-area, S-cone-driven squares in participants P2 and P4 were small and peaked later in time than the large-area L-M-driven responses drawn in Figure 5. Because they were observable only in two of the eight participants who gave measurable cVEPs for stimuli in the L-M direction, we could not perform population analyses of the large-area S-cone-driven data. Note that the lack of S-cone responses for uniform stimuli may tie into results showing that only the L-M component of color contributes to equiluminant motion processing except under specific stimulus parameters (Ruppertsberg et al., 2007); it was also suggested that early extraction of color signal may act as a cue to facilitate subsequent motion processing (Martinovic et al., 2009), so the lack of an early S-cone response could perhaps explain why S-cone signals are invisible to the motion system. The remainder of the Results section is about quantitative analysis of cVEPs to stimuli in the L-M and Red directions.

Quantitative analysis of cVEPS across the participant population

Amplitude

First, we studied the amplitude of cVEPs to large-area stimuli and its dependence on cone-contrast. Amplitude data for cVEPs to color-complement checkerboards and to large-area squares are plotted in Figure 7. The data points in Figure 7 are the medians of the peak amplitude of the populations of participants studied for each stimulus condition. It is evident that response amplitudes of the cVEPS evoked by the square stimuli were much smaller than the checkerboard responses, which is consistent with the examples in Figures 4 and 5. Also, it is interesting that the response amplitudes to L-M and Red stimuli overlapped when plotted versus L-M conecontrast.

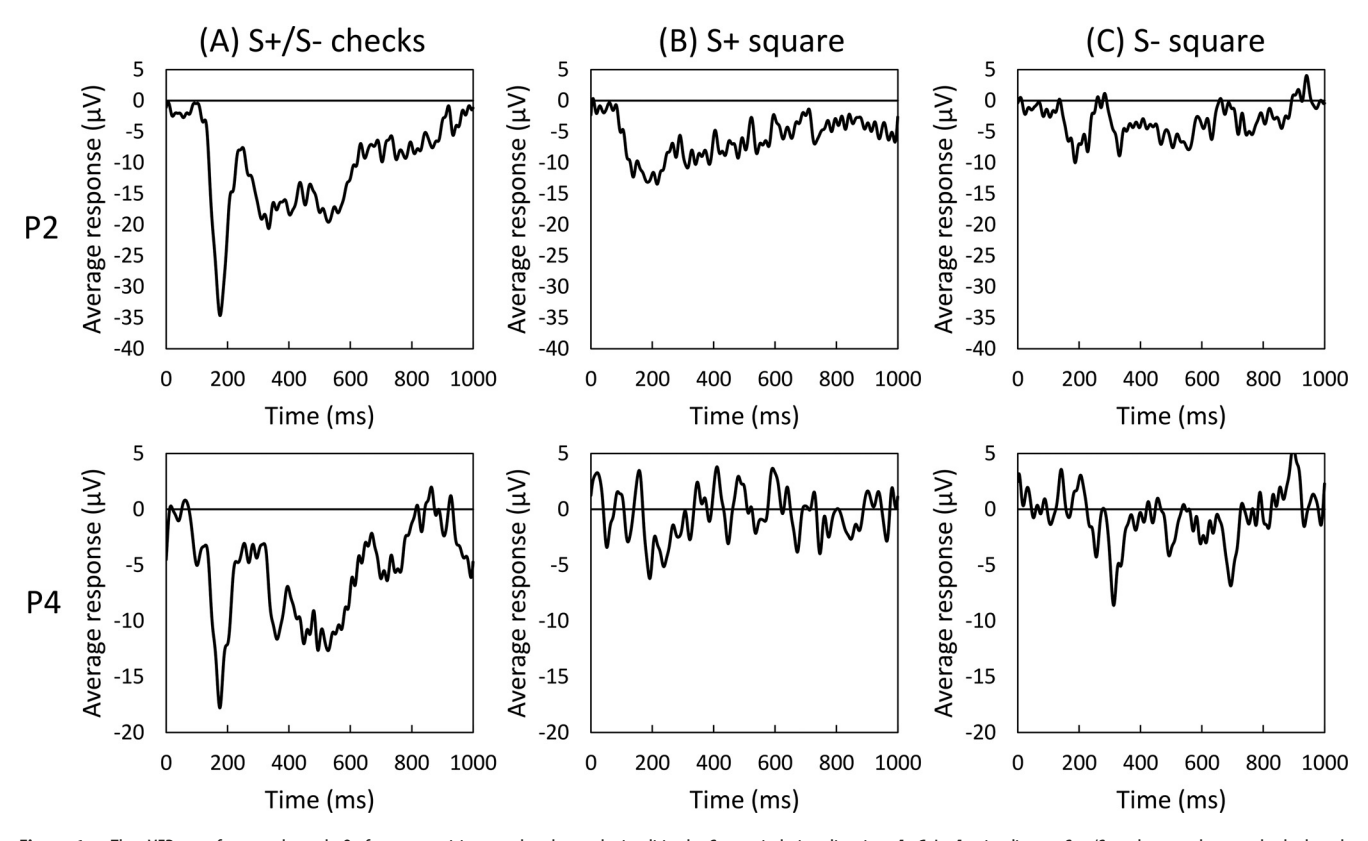


Figure 6. The cVEP waveform at electrode 0z for two participants who observed stimuli in the S-cone-isolating direction. A-C, In A, stimuli were S+/S- color-complement checkerboards; in B, the stimuli were uniform squares in the S+ direction; and in C, the stimuli were uniform squares in the complementary S- direction. While participant P2 shows small peaks at \sim 200 ms for the uniform squares, the corresponding responses for participant P4 are less evident.

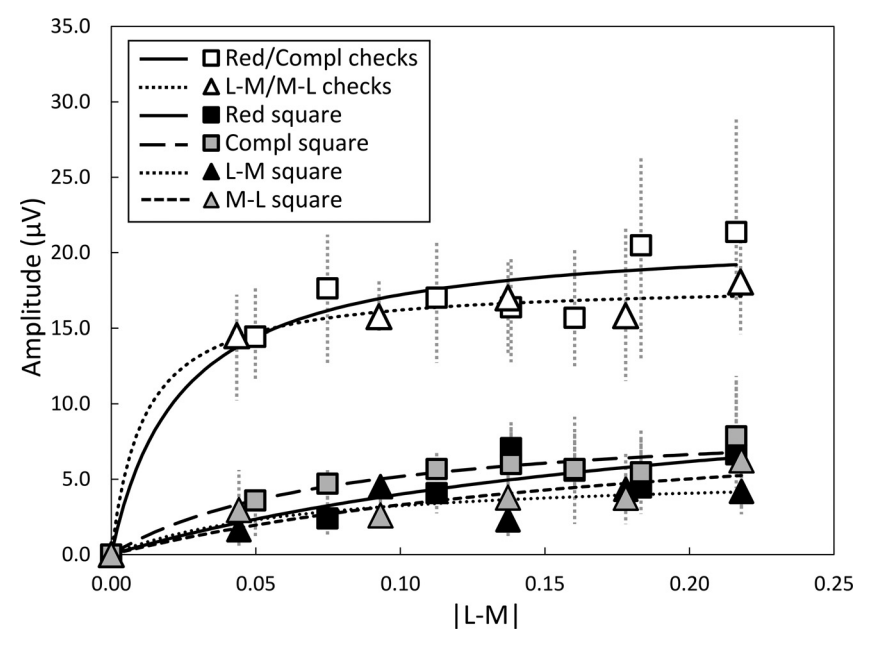


Figure 7. Median peak amplitude of the participants plotted as a function of contrast measure |L-M| for the color-complement checkerboard and uniform-square stimuli in the L-M and Red color directions. The interquartile range of each data point is represented by gray vertical dotted lines. A value of zero response at zero contrast was added for each color direction. Naka—Rushton curves were fitted through each set of data using the method of least squares.

We analyzed the amplitude data to determine the significance of the difference between the responses to squares and checkerboards. The quantity analyzed was the peak amplitude of the earliest negative peak of waveforms like those shown in Figures 4 and 5. We compared the amplitude vs cone contrast function of the population to large-area stimuli with that of cVEP responses to color-complement checkerboards to test the hypothesis that the large-area stimuli were mostly driving Single-Opponent cells while color-complement checkerboard stimuli were most effective in activating Double-Opponent cells.

Statistical analysis revealed that large-area cVEP amplitudes are significantly smaller than the amplitudes of the checkerboard responses in both L-M and Red color directions (Fig. 7). First, to improve the signal-to-noise ratio for the noisier large-area cVEPs, we averaged the large-area data for color and complement in each color direction. Then we did a two-way repeated-measures ANOVA for contrast × pattern, for each color direction in JASP (version 0.16). For L-M, there was a significant main effect of pattern ($F_{(1,4)} = 23.633$, p =0.008). In addition, there was a very large effect size ($\eta^2 = 0.755$) because the amplitudes of the checkerboard responses were much bigger. There also was a significant main effect of contrast ($F_{(4,16)} = 4.575$, p = 0.012), but this had a small effect size ($\eta^2 = 0.039$), and there was no significant interaction. Note that for this

ANOVA, the datasets from three participants were rejected for not having data for every contrast in both patterns, but the results were still strong for the five participants included in the test. For the Red direction, again with five participants included, in the ANOVA there was a significant main effect of pattern ($F_{(1,4)}=14.304, p=0.019$) and, again, a very large effect size ($\eta^2=0.695$) because the amplitudes of the checkerboard responses were much bigger. There was a significant main effect of contrast ($F_{(4,16)}=4.868, p=0.009$) and a small effect size ($\eta^2=0.030$), and there was no significant interaction.

The dependence of response amplitudes on cone-contrast was very weak, for both large-area squares and for color-complement checkerboards, as indicated by the small effect sizes in the ANOVA. It is worth noting that the slope of the amplitude versus cone-contrast curve of the checkerboard responses was less than we reported recently for the same dataset (Nunez et al., 2021). This is because of different treatments of the same checkerboard data. For this article, we filtered all the cVEP waveforms to be within the 0-50 Hz band, while Nunez et al. (2021) used a 0-100 Hz bandwidth. We found that the waveforms filtered through the wider bandwidth were noisier and that the optimal signal band was 0-50 Hz. The noisier waveforms used in the Nunez et al. (2021) study yielded a somewhat larger slope for the amplitude versus cone-contrast functions, but we think that the shallower slopes of the checkerboard amplitude versus conecontrast data shown here (Fig. 7) are more accurate.

Next, we turn to the comparison of response amplitudes in the L-M and Red color directions, focusing on the amplitudes of responses to large-area squares. We analyzed the data to find out whether or not there was a significant difference between the L-M and Red color directions in the dependence of their peak amplitudes on cone-contrast and found no difference for the large-area responses. Specifically, we calculated the slope and intercept for color-complement-averaged large-area data for each participant, without including a zero value at zero contrast (and using the L-M contrast for both the L-M direction and the Red direction). Then we used the revised t-statistic of the study by Derrick et al. (2017), which was created specifically for partially overlapping data, to compare the slope and intercepts of L-M versus Red for large-area stimuli. There was no significant difference between L-M and Red slopes of amplitude versus conecontrast (p = 0.166). Also, there was no significant difference between L-M and Red intercepts (p = 0.787). That is, with respect to peak amplitudes, the cVEPs of the L-M and Red directions are not significantly different.

We applied the same t-test analysis to the checkerboard data and found that there was no significant difference between L-M and Red checkerboard slopes (p=0.615) or intercepts (p=0.415), which is consistent with our earlier analyses of L-M and Red checkerboard data (Nunez et al., 2021).

To summarize, response amplitudes of the large-area square stimuli are much smaller than for color checkerboards, and there is very little change in response amplitude with cone-contrast for both kinds of stimuli. It is conceivable that the amplitude difference between cVEPs evoked by checkerboard and large-area squares could reflect the spatial tuning of a single neuronal population of Double-Opponent cells, which are more activated by checkerboards than by the large-area squares. The results about the latency of responses, presented next, tend to rule out the single-population hypothesis.

Latency

By latency, we mean the time to peak negativity of the earliest deflection of the average EEG in response to the appearance of the color stimuli. This is a different definition from what we used before (Nunez et al., 2021); previously when studying cVEPs in

response to checkerboard appearance, we defined latency as the time between the onset of pattern appearance and the time when the earliest negative deflection of the cVEP reached 75% of its peak value. Because the cVEPs to large-area squares were much smaller and therefore noisier than the checkerboard responses (Fig. 7), it was necessary to use the time to peak as the criterion here.

The latencies of the cVEPs evoked by large-area squares were consistently much less than the latencies of responses to checkerboards (Fig. 8A,B). Plotted in Figure 8 are the average latencies across the populations of observers that viewed the L-M and the Red stimuli. It is obvious that the color-checkerboard latency was larger than the latency of response to the large-area squares at all values of cone-contrast. In Figure 8A, the latency data are plotted versus cone-contrast defined as $\sqrt{(L-M)^2+S^2}$, the vector sum of the L-M and S cone-contrasts. This vector sum simply equals L-M contrast for the L-M stimuli that have zero S-conecontrast, but it includes the nonzero S-cone-contrast for the Red stimuli. In Figure 8B, the same latency data are plotted versus L-M contrast only. The data overlap when plotted versus L-M cone-contrast, which is consistent with the idea that it is L-M cone-contrast that determines the latency of the peak response for cVEPs both to color checkerboards (Nunez et al., 2021) and to large-area squares of color.

To compare the checkerboard and squares data statistically, we conducted t-tests to compare the latencies for large-area squares and checkerboards at high cone-contrast where the checkerboard latency occurs at the asymptotes (Fig. 8). We used the maximum cone-contrast available in the L-M direction (|L-M contrast = 0.218) and the second highest contrast in the Red direction (|L-M| contrast = 0.183) because not all participants had a Red complement within the gamut for the highest contrast (a result of individual differences in HFP responses). We used repeated-measures *t*-tests in both the L-M and Red directions. There was no significant difference between the latencies for color and complement uniform-square stimuli in either color direction, and so we averaged the color (L-M, Red) and complement (M-L, Red-complement) large-square data. Then we used a dependent t-test to compare the (high-contrast) latency for large-area squares with that of checkerboards. In the L-M color direction, the mean checkerboard latency (mean = 132.6 ms, SEM = 4.4 ms) was significantly greater than the mean large-area square latency (mean = 84.4 ms, SEM = 1.9 ms; $t_{(7.0)}$ = 13.043, p < 0.001). In the Red color direction, we had to use the t-test in the study by Derrick et al. (2017) that was modified for overlapping samples and unequal samples sizes. In the Red direction, the mean checkerboard latency (mean = 131.8 ms, SEM = 5.6 ms) also was significantly greater than the mean large-area square latency (mean = 86.3 ms, SEM = 1.9 ms; $t_{(8.8)}$ = 7.446, p < 0.001). The large and significant latency differences between responses to the two kinds of visual stimuli at high cone-contrast supports the hypothesis that the neuronal mechanism that is generating cVEPs to large-area color squares is distinct from the mechanisms that are responding to color-checkerboard patterns in the L-M and Red color directions.

Even more striking than the difference in the latencies at high cone-contrast, the cone-contrast dependences of latencies appear qualitatively different for cVEPs to large-area stimuli versus checkerboards (Fig. 8). For checkerboard-evoked cVEPs, there is a large progressive decrease in latency with increasing cone-contrast, as has been reported before (Murray et al., 1987; Rabin et al., 1994; Crognale, 2002; Souza et al., 2008; Nunez et al., 2017,

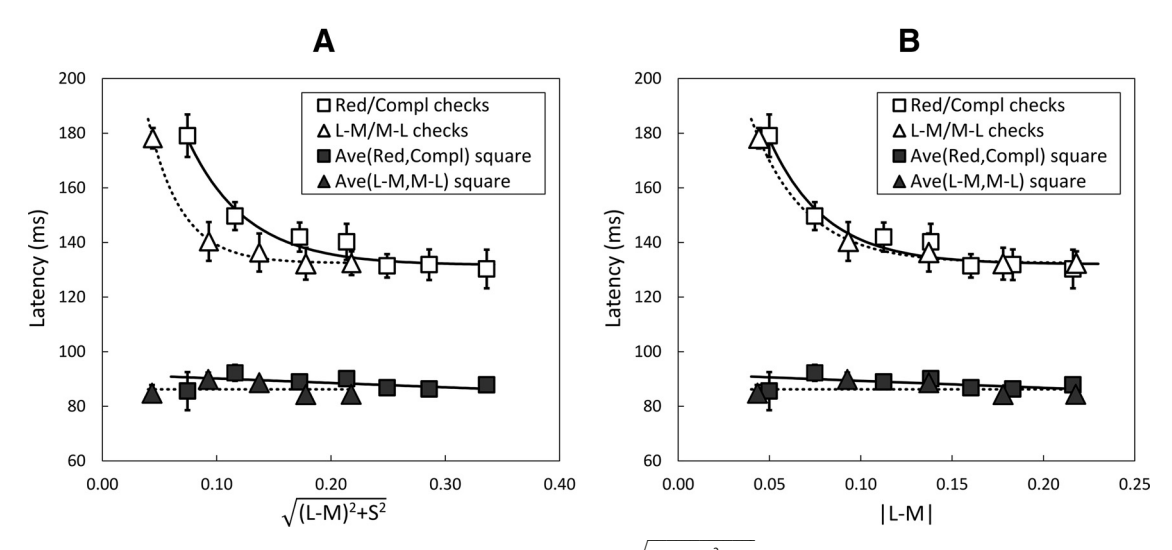


Figure 8. A, B, Grand-averaged latency plotted as a function of the following: contrast measure $\sqrt{(L-M)^2+5^2}$ (A) and contrast measure |L-M| (B) for the color-complement checkerboard and for the uniform-square stimulus. The latencies of the peak for the color and complement uniform squares were averaged for each contrast. For both the L-M and Red color directions, the latency of the color-complement checkerboard (gray symbols) is initially quite high but decreases as the contrast increases. However, the latency of the peak for the uniform square is relatively independent of contrast. Latency was defined as the time taken from stimulus onset to reach the peak amplitude of response. Error bars represent ± 1 SEM. For points without visible error bars, the error bars are smaller than the symbols.

2018). Over the range of cone-contrast we used, the latency of the checkerboard cVEP dropped by 45 ms, from 180 to 135 ms, for both L-M and Red color directions. However, it is very different for the latency of the cVEPs evoked by the large-area squares; it changed little with increasing cone-contrast, dropping from a mean value of 89 ms at a cone-contrast of 0.05 to 85 ms at a cone-contrast of 0.22. There is little difference between L-M and Red color directions in this regard. Another way of quantifying the difference is by calculating the percentage change in latency from low to high cone-contrast. For the L-M checkerboards, there was a 31.9% reduction in latency, while for Red checkerboards the decrease was 34.0%. The percentage decrease of latency with increasing cone-contrast for large area squares was much smaller: L-M squares, 6.4%; Red squares, 7.6%.

We also calculated the statistical significance of the difference in the cone-contrast dependence of the latencies. First, we analyzed the latency data for the large-area squares comparing the latency dependences on contrast of different color directions. For this comparison, we used a two-way repeated-measures ANOVA of color direction and contrast. The ANOVA showed no significant effect of color direction when the L-M and M-L directions were compared. However, when Red and Red complement were compared, there was a significant main effect of color direction ($F_{(1,4)} = 10.771$, p = 0.030). The difference between Red and Red-complement latencies was small (contrast-averaged difference <3 ms) compared with the latencies themselves, which ranged from 85 to 95 ms. Therefore, we thought it would be reasonable to average the color and complement square latencies in each color direction when we did a statistical comparison of large-area and checkerboard latency data.

Then we used a two-way pattern \times contrast repeated-measures ANOVA on latencies for color-complement-averaged uniform-square and color-complement checkerboards. There were significant main effects of pattern and contrast, as well as a significant interaction, in both the Red and L-M color directions (Table 2, ANOVA statistics).

The large main effects of pattern and the interactions of pattern and contrast in the ANOVA confirm what appears evident in Figure 8, namely that the change in latency with cone-contrast

Table 2. Summary of statistics from the two-way pattern \times contrast ANOVA for latency data presented as a function of contrast in Figure 8

•	•	•
	L-M direction	Red direction
Main effect of pattern	$F_{(1,5)} = 414.3, p < 0.001,$ $\eta^2 = 0.751$	$F_{(1,3)} = 352.2, p < 0.001,$ $\eta^2 = 0.769$
Main effect of contrast	$F_{(4,20)} = 21.5, p < 0.001,$ $\eta^2 = 0.085$	$F_{(5,15)} = 11.6, p < 0.001,$ $\eta^2 = 0.101$
Interaction	$F_{(1.68,8.40)} = 18.8^*, p = 0.001,$ $\eta^2 = 0.107$	$F_{(5,15)} = 6.7, p = 0.002,$ $\eta^2 = 0.067$

The patterns were uniform-square or color-complement checkerboards. The contrasts were the L-M component of contrast for both L-M and Red stimuli. Separate ANOVAs were performed in the L-M and Red color directions because the datasets did not have the same contrasts.

*For the pattern-contrast interaction term in the L-M direction, Mauchly's test of sphericity indicated that the sphericity assumption was violated, so the Greenhouse–Geisser correction was used. The effect sizes are given by η^2 .

is significantly smaller for squares versus checkerboards. These results further support the hypothesis that different neuronal chromatic mechanisms are responding respectively to checkerboard patterns and to large-area squares.

Transientness

The shapes of the cVEP waveforms of responses to large-area squares in Figures 4 and 5 are different from the waveforms of the responses to checkerboards. One quantitative measure of this difference is the transientness of the waveform. As has been done previously (Nunez et al., 2021), we defined transientness as follows:

Transientness =
$$\{V(t_{peak}) - \langle V(t) \rangle_{300-500ms}\}/V(t_{peak})$$
.

For a completely sustained response, transientness = 0. For a response that relaxes back from a peak value to 0 before 300 ms, transientness = 1. The transientness of L-M and Red large-area squares are compared with each other and with the transientness of L-M/M-L and Red/Red-Compl checkerboards in Figure 9. The transientness data were analyzed with *t*-tests applied to paired comparisons of large-area squares versus checks and of large-area L-M versus Large-area Red. The results are summarized in Table 3. From the bar graphs in Figure 9 and Table 3, one

can observe that the cVEPs to large-area stimuli were generally more transient than checkerboard responses, a result possibly related to the results of Martinovic et al. (2011). In addition, there was no significant difference in transientness between L-M and Red for the large-area stimuli. This last result is most salient because it is consistent with the hypothesis that a single neuronal mechanism is generating the large-area response to both L-M and Red.

Discussion

Single-Opponent cells

We propose the following interpretation of the Results: that a distinct neuronal mechanism, namely the population of Red-Green Single-Opponent cortical cells in V1, is responsible for the cVEPs evoked by the appearance of large-area, equiluminant-color squares; and that cVEP responses to a color checkerboard are the results of the activation of Double-Opponent color neurons, as postulated previously (Nunez et al., 2017, 2018, 2021; Shapley et al., 2019).

One reason for our Single-Opponent proposal is based on prior work on the spatial tuning of V1 neurons. Single-Opponent neurons have distinct visual properties from those of the more numerous Double-Opponent color cells that comprise the larger fraction of cells in V1 that respond to equiluminant color stimuli. Single-Opponent cells respond to spatially diffuse color stimuli like equiluminant spatial grating patterns of low spatial frequency and blobs of equiluminant color. Neurons in the Single-Opponent population would be the most likely to respond to largearea, equiluminant-color squares of the kind that we used in our experiments. The other neuronal populations that have been studied in V1 cortex, Non-Opponent cells and Double-Opponent cells, would not be expected to respond to equiluminant-color, large-area squares. Non-Opponent cells are by definition poorly responsive to equiluminant-color stimuli. Double-Opponent cells respond to equiluminant-color but only weakly if at all to stimuli like large-area squares because the Double-Opponent neurons are spatially tuned (Thorell et al., 1984; Johnson et al., 2001, 2008; Schluppeck and Engel, 2002; Conway et al., 2010). Thus, it is reasonable to believe that the cVEPs to large-areas of color are the activity of Single-Opponent cells. A reviewer suggested a control experiment to support this: starting with an equiluminant large area square, we increased luminance while decreasing L-M contrast. Data from the one participant we tested were unequivocal: VEP response was maximal for L-M equiluminant stimuli, thereby ruling out Non-Opponent cells as its source. Similarly, Paulus et al. (1984) added luminance contrast to a color disk and found that for a VEP peak of latency 87 ms, amplitude varied very little with luminance contrast. These experiments are consistent with our suggestion that large, uniform color stimuli evoke responses from a color-opponent neural mechanism, namely the population of Single-Opponent cortical cells.

Second, the amplitudes and latencies of responses to largearea squares were very different from those to color checkerboards (Figs. 4, 5, 7, 8). The large and significant differences are consistent with the hypothesis that the two different kinds of spatial stimulus revealed two distinct types of neuronal mechanisms.

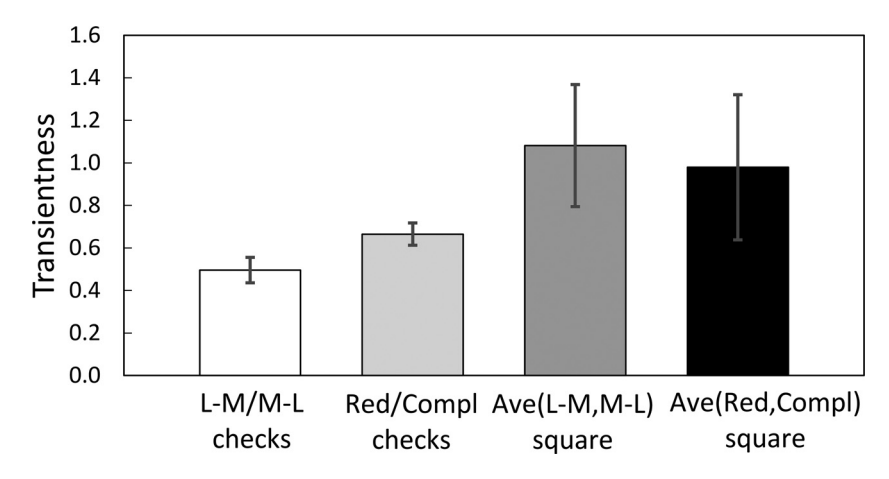


Figure 9. Transientness averaged over each contrast range for the color-complement checkerboards in the L-M and Red color directions and for the L-M and Red uniform square stimuli. The contrast-averaged transientness for each participant was converted to a grand average for each color direction. For the uniform squares, as there was no significant difference between transientness of color and complement, they were averaged together for each color direction. For the L-M and Red squares, N = 8; for the L-M/M-L checkerboard, N = 7; and for the Red/complement checkerboard direction, N = 14. Transientness was defined as the difference between the peak amplitude and the average response over 300–500 ms poststimulus, normalized by the peak amplitude. Error bars represent ± 1 SEM.

Table 3. Summary of t-test results comparing contrast-averaged transientness in the L-M versus Red color directions for a large-area square and a color-complement checkerboard, as well as comparing transientness for the square versus color-complement checkerboard in each of the L-M and Red color directions

Comparison of transientness means	<i>t</i> -statistic	df	<i>p</i> -Value
Red vs L-M directions, large-area square	0.338	7.75	0.372
Red vs L-M directions, color-Compl checkerboard	2.984	8.62	0.009
Square vs color-Compl checkerboard, L-M direction	2.490	6.47	0.024
Square vs color-Compl checkerboard, Red direction	0.985	5.76	0.185

The t-tests were modified for overlapping datasets using the method of Derrick et al. (2017). For the squares, as there was no significant difference between Transientness of color and complement, color and complement transientness were averaged together for each color direction. There was no significant difference in Transientness between the L-M and Red directions for the large-area squares but responses to Red/complement cl. (2011).

Third, cVEPs evoked by large-area squares had only a small change in response latency across a large range of cone-contrast (Fig. 8). It is well known from previous studies that the latencies of responses to color checkerboards are strongly dependent on cone-contrast (Murray et al., 1987; Rabin et al., 1994; Crognale, 2002; Souza et al., 2008; Nunez et al., 2017, 2018), as we confirmed (Fig. 8). In our data, the average reduction of latency to color checkerboards over the range of cone-contrast from 0.04 to 0.33 was 33%. Previously, we proposed that such strong dependence of cVEP latency on cone-contrast was evidence of nonlinear cortical dynamics that affected the responses of Double-Opponent cells (Nunez et al., 2017). The weak dependence of latency on cone-contrast for the responses to large-area squares is quite different from that for color-checkerboard patterns (Fig. 8). After averaging across L-M and Red directions, the percentage change of the cVEP latency to squares was only 7%. The much weaker cone-contrast dependence could be the dynamic signature of the Single-Opponent population. In terms of latency, the response dynamics of the putative Single-Opponent signal is more linear than that of the Double-Opponent signals (Fig. 8), though the amplitudes of cVEPs to both color checkerboards and large-area color squares had nonlinear (saturating) dependences on conecontrast (Fig. 7).

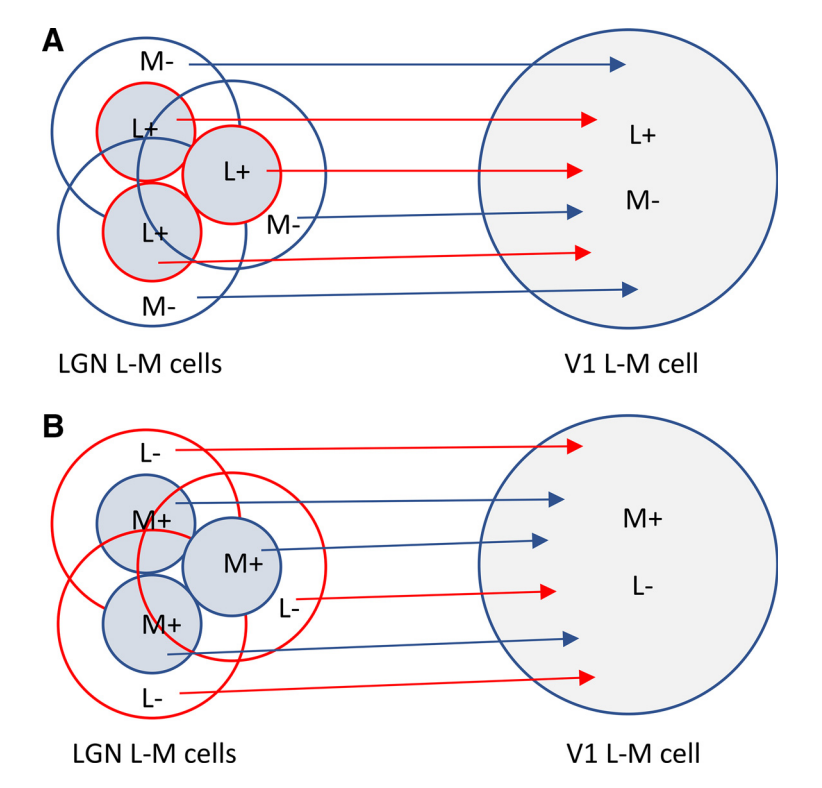


Figure 10. Model indicating how the receptive fields of single-opponent neurons in the LGN may project to single-opponent neurons in the cortex. **A**, In the LGN, an L-M single-opponent cell has a center excited by increments in L-cone contrast, and a surround excited by decrements in M-cone contrast. Multiple LGN cells project to larger single-opponent cells in the early visual cortex so that in V1 the L+ center and M- surround are coextensive. **B**, Similarly, M-L cells with centers excited by M-cone increments and surround excited by L-cone decrements project to coextensive larger M-L neurons in V1. Note that these single-opponent receptive fields correspond to the type Il LGN cells of Wiesel and Hubel (1966), and to the "Center-only opponent" receptive field model in the study by Conway et al. (2010, their Fig. 3*B*).

L-M (M-L) Single-Opponent cells

A second hypothesis is that the Single-Opponent cells in human V1 are homogeneous in their color properties. That is, we interpret the data (Figs. 7-9) to mean that the activity of the Single-Opponent population that our experiments measured is mostly driven by signals along the L-M cardinal direction of color space. Our interpretation is supported by the similarity of amplitude, latency, and transientness in the color directions we studied: L-M and Red.

Note that the results on color checkerboards are different. Here (Fig. 9) and in an earlier study (Nunez et al., 2021), we showed that transientness is significantly different for checkerboard-evoked cVEPs in the L-M and Red directions. The results for checkerboards suggest that there are many different kinds of Double-Opponent cells with different color properties (Nunez et al., 2021). Others who studied human cVEPs with experimental paradigms different from ours reached similar conclusions about the heterogeneity of the color properties of spatially-tuned color cells in humans (Kaneko et al., 2020; Chen and Gegenfurtner, 2021).

The hypothesis of Single-Opponent color homogeneity is consistent with results on single-cell neurophysiology in macaque V1 (Lennie et al., 1990; Johnson et al., 2004; Solomon and Lennie, 2005). The neurophysiology indicated that the optimal color directions for the activation of V1 Single-Opponent cells are clustered around the L-M cardinal direction, while the population of spatially tuned, color-responsive neurons (that we have

called Double-Opponent) has a broader distribution of optimal color directions.

Much more research needs to be done to understand how the different color responses of color-responsive neurons in primate V1 cortex are manufactured by the cortical circuitry. We offer a sketch of a possible wiring diagram for the L-M (or M-L) Single-Opponent cells in Figure 10. The basic idea of the diagram is that several Single-Opponent LGN neurons of the same color type (L-M or M-L) could converge onto one cortical Single-Opponent cell. That would explain both the somewhat larger receptive fields of cortical Single-Opponent cells compared with the small receptive fields of LGN cells, and also the clustering of optimal color directions of Single-Opponent cells near the L-M cardinal direction in the cortical population (Derrington et al., 1984; Lennie et al., 1990; Johnson et al., 2004; Solomon and Lennie, 2005).

Are there S-cone-driven Single-Opponent cells?

As reported in Results, in most participants tested there was no measurable cVEP to a large-area square modulated in the S-cone cardinal direction of color space. In two participants, we found small S-cone-driven cVEPs (Fig. 6), but they were small and noisy responses. Also, even in the two participants who did produce S-cone-driven cVEPs to squares, their responses to squares were much smaller than their responses to S+/S- checkerboards (Fig. 6, left panels). These negative results with S-cone-driven cVEPS suggest that

there may be few S-cone-driven Single-Opponent neurons in human visual cortex. Such a conclusion is consistent with macaque neurophysiology; very few if any V1 Single-Opponent cells that receive substantial S-cone drive have been reported (Lennie et al., 1990; Johnson et al., 2004; Solomon and Lennie, 2005).

The situation is different for Double-Opponent cells. Many macaque V1 neurons that are spatially tuned for color receive S-cone excitation (Lennie et al., 1990; Johnson et al., 2004; Solomon and Lennie, 2005). Consistent with the single-cell neurophysiology, S-cone signals evoked by color checkerboards are effective in producing human cVEPs (Nunez et al., 2021), which are shown in Figure 6, left panels. One must infer that the S-cone signals carried by the koniocellular pathway to V1 are routed mostly, if not exclusively, to the Double-Opponent population. These results suggest that the L-M and S cardinal directions are treated differently in the visual cortex. L-M signals are sent to both Single-Opponent and Double-Opponent cells, but S-cone signals seem to be sent to Double-Opponent cells preferentially.

Are there other sources of the cVEPs to large color squares?

The schematic diagram presented in Figure 10 for the generation of Single-Opponent cells in V1 cortex is based on the presumption that these cortical neurons are driven by parvocellular Single-Opponent cells. It is well known that the largest number of afferent inputs to V1 comes from

the parvocellular layers of the LGN, and most of those neurons are L-M or M-L opponent cells (De Valois, 1960; Derrington et al., 1984; Chatterjee and Callaway, 2003). The cVEP signals that we assign to the Single-Opponent cell population also are driven only by L-M or M-L conecontrast, with very weak or no S-cone input. Therefore, it seems to us that a parvocellular source of activation is likely. One might ask, is it possible that the Single-Opponent cells that respond to the equiluminant large-area squares could derive their excitatory drive from other sources? The only other input that has the right cone weights might be the frequency-doubled responses to equiluminant color modulation of low spatial frequency patterns or large areas of color observed in Magnocellular neurons (Lee et al., 1989). However, the Magnocellular LGN color response amplitudes are highly dependent on cone-contrast (Lee et al., 1989) and Magnocellular LGN signals are known to speed up with contrast (Benardete et al., 1992). Extending the macaque Magnocellular results to the human cortex by using conditions that favored the M pathway (i.e., low achromatic contrast), Zemon and Gordon (2006) found a decrease in achromatic VEP phase with increasing contrast. That is, the response sped up with increasing contrast (Zemon and Gordon, 2006). These Magnocellular characteristics make it unlikely that Magnocellular neurons are the sources of activation of the cortical Single-Opponent cVEPs that have very flat amplitude versus contrast functions (Fig. 7) and latency that varies very little with contrast (Fig. 8).

References

- Benardete EA, Kaplan E, Knight BW (1992) Contrast gain control in the primate retina: p cells are not X-like, some M cells are. Vis Neurosci 8:483–486
- Brainard D (1996) Cone contrast and opponent modulation color spaces. In: Human color vision (Kaiser PK, Boynton RM, eds), pp 563–579. Washington, DC: Optical Society of America.
- Brainard DH (1997) The Psychophysics toolbox. Spat Vis 10:433-436.
- Brainard DH (2004) Color constancy. In: The visual neurosciences (Chalupa LM, Werner JS, eds), pp 948–961. Cambridge, MA: MIT.
- Chatterjee S, Callaway EM (2003) Parallel colour-opponent pathways to primary visual cortex. Nature, 426:668–671.
- Chen J, Gegenfurtner KR (2021) Electrophysiological evidence for higher-level chromatic mechanisms in humans J Vis 21(8):12, 1–14.
- Cohen-Duwek H, Spitzer H (2019) A compound computational model for filling-in processes triggered by edges: watercolor illusions. Front Neurosci 13:225.
- Conway BR, Chatterjee S, Field GD, Horwitz GD, Johnson EN, Koida K, Mancuso K (2010) Advances in color science: from retina to behavior. J Neurosci 30:14955–14963.
- Crognale MA (2002) Development, maturation, and aging of chromatic visual pathways: VEP results. J Vis 2(6):438–450.
- Crognale MA, Duncan CS, Shoenhard H, Peterson DJ, Berryhill ME (2013) The locus of color sensation: cortical color loss and the chromatic visual evoked potential. J Vis 13(10):15, 1–11.
- Derrick B, Russ B, Toher D, White P (2017) Test statistics for the comparison of means for two samples that include both paired and independent observations. J Mod Appl Stat Methods 16:137–157.
- Derrington AM, Krauskopf J, Lennie P (1984) Chromatic mechanisms in lateral geniculate nucleus of macaque. J Physiol 357:241–265.
- De Valois RL (1960) Color vision mechanisms in the monkey. J Gen Physiol 43 [Suppl 6]:115–128.
- De Valois RL, De Valois KK (1988) Spatial vision. New York: Oxford UP.
- Devinck F, Knoblauch K (2019) Central mechanisms of perceptual filling-in. Curr Opin Behav Sci 30:135–40.
- Devinck F, Gerardin P, Dojat M, Knoblauch K (2014) Spatial selectivity of the watercolor effect. J Opt Soc Am A Opt Image Sci Vis 31:A1–A6.

- Foster DH (2011) Color constancy. Vision Res 51:674-700
- Friedman HS, Zhou H, von der Heydt R (2003) The coding of uniform colour figures in monkey visual cortex. J Physiol 548:593–613.
- Garg AK, Li P, Rashid MS, Callaway EM (2019) Color and orientation are jointly coded and spatially organized in primate primary visual cortex. Science 364:1275–1279.
- Girard P, Morrone MC (1995) Spatial structure of chromatically opponent receptive fields in the human visual system. Vis Neurosci 12:103-116.
- Hass CA, Horwitz GD (2013) V1 mechanisms underlying chromatic contrast detection. J Neurophysiol 109:2483–2494.
- Johnson EN, Mullen KT (2016) Color in the cortex. In: Human color vision (Kremers J, Baraas RC, Marshall NJ, eds), pp 189–218. Cham, Switzerland: Springer.
- Johnson EN, Hawken MJ, Shapley R (2001) The spatial transformation of color in the primary visual cortex of the macaque monkey. Nat Neurosci 4:409–416.
- Johnson EN, Hawken MJ, Shapley R (2004) Cone inputs in macaque primary visual cortex. J Neurophysiol 91:2501–2514.
- Johnson EN, Hawken MJ, Shapley R (2008) The orientation selectivity of color-responsive neurons in macaque V1. J Neurosci 28:8096– 8106.
- Kaneko S, Kuriki I, Andersen SK (2020) Steady-state visual evoked potentials elicited from early visual cortex reflect both perceptual color space and cone-opponent mechanisms. Cereb Cortex Commun 1:tgaa059.
- Kiper DC, Levitt JB, Gegenfurtner KR (2001) Chromatic signals in extrastriate areas V2 and V3. In: Color vision, from genes to perception (Gegenfurtner KR, Sharpe LT, eds), pp 249–268. Cambridge, UK: Cambridge UP.
- Kleiner M, Brainard D, Pelli D, Ingling A, Murray R, Broussard C (2007) What's new in Psychtoolbox-3. Perception 36:1–16.
- Krauskopf J (1963) Effect of retinal image stabilization on the appearance of heterochromatic targets. J Opt Soc Am 53:741–744.
- Lee BB, Martin PR, Valberg A (1989) Nonlinear summation of M-and L-cone inputs to phasic retinal ganglion cells of the macaque. J Neurosci 9:1433–1442.
- Lennie P, Krauskopf J, Sclar G (1990) Chromatic mechanisms in striate cortex of macaque. J Neurosci 10:649–669.
- Livingstone MS, Hubel DH (1984) Anatomy and physiology of a color system in the primate visual cortex. J Neurosci 4:309–356.
- Martinovic J, Meyer G, Müller MM, Wuerger SM (2009) S-cone signals invisible to the motion system can improve motion extraction via grouping by color. Vis Neurosci 26:237–48.
- Martinovic J, Mordal J, Wuerger SM (2011) Event-related potentials reveal an early advantage for luminance contours in the processing of objects. J Vis 11(7):1, 1–15.
- Murray IJ, Parry NRA, Carden D, Kulikowski JJ (1987) Human visualevoked potentials to chromatic and achromatic gratings. Clin Vis Sci 1:231–244.
- Nunez V, Shapley RM, Gordon J (2017) Nonlinear dynamics of cortical responses to color in the human cVEP. J Vis 17(11):9, 1–13.
- Nunez V, Shapley RM, Gordon J (2018) Cortical double-opponent cells in color perception: perceptual scaling and chromatic visual evoked potentials. Iperception 9:2041669517752715.
- Nunez V, Gordon J, Shapley RM (2021) A multiplicity of color-responsive cortical mechanisms revealed by the dynamics of cVEPs. Vision Res 188:234–245.
- Paulus WM, Hömberg V, Cunningham K, Halliday AM, Rohde N (1984) Colour and brightness components of foveal visual evoked potentials in man Electroenceph Clin Neurophysiol 58:107–119
- Pelli DG (1997) The VideoToolbox software for visual psychophysics: transforming numbers into movies. Spat Vis 10:437–442.
- Rabin J, Switkes E, Crognale M, Schneck ME, Adams AJ (1994) Visual evoked potentials in three-dimensional color space: correlates of spatiochromatic processing. Vision Res 34:2657–2671.
- Ruppertsberg AI, Wuerger SM, Bertamini M (2007) When S-cones contribute to chromatic global motion processing. Vis Neurosci 24:1–8.
- Schluppeck D, Engel SA (2002) Color opponent neurons in V1: a review and model reconciling results from imaging and single-unit recording. J Vis 2:480–492.

- Shapiro A, Hedjar L, Dixon E, Kitaoka A (2018) Kitaoka's tomato: two simple explanations based on information in the stimulus. Iperception 9:2041669517749601.
- Shapley R, Nunez V, Gordon J (2019) Cortical double-opponent cells and human color perception. Curr Opin Behav Sci 30:1–7.
- Solomon SG, Lennie P (2005) Chromatic gain controls in visual cortical neurons. J Neurosci 25:4779–4792.
- Souza GS, Gomes BD, Lacerda EM, Saito CA, da Silva Filho M, Silveira LC (2008) Amplitude of the transient visual evoked potential (tVEP) as a function of achromatic and chromatic contrast: contribution of different visual pathways. Vis Neurosci 25:317–325.
- Thorell LG, de Valois RL, Albrecht DG (1984) Spatial mapping of monkey VI cells with pure color and luminance stimuli. Vision Res 24:751–769.
- Wiesel TN, Hubel DH (1966) Spatial and chromatic interactions in the lateral geniculate body of the rhesus monkey. J Neurophysiol 29:1115–1156.
- Wuerger SM, Atkinson P, Cropper S (2005) The cone inputs to the uniquehue mechanisms. Vision Res 45:3210–3223.
- Zemon V, Gordon J (2006) Luminance-contrast mechanisms in humans: visual evoked potentials and a nonlinear model. Vision Res 46:4163–4180